

DISTRIBUTION OF TRAPPED GAS SATURATION IN HETEROGENEOUS SANDSTONE RESERVOIRS

SUZANNE Karine (Ecole des Mines de Paris), HAMON Gérald (TotalFinaElf),
BILLIOTTE Joël (Ecole des Mines de Paris), TROCME Vincent (GazDeFrance)

ABSTRACT

Maximum residual gas saturation (S_{grm}) is known to be a key factor in evaluating gas recovery from a lean gas reservoir invaded by aquifer water. This work focuses on variations of S_{grm} within heterogeneous gas-bearing sandstone reservoirs.

Three hundred S_{grm} measurements were performed by capillary imbibition and supplemented by lithological description, thin sections, XRD analysis, porosity, permeability, grain density, formation factor and cementation factor. The core plugs were selected from three different sandstone gas reservoirs and from Fontainebleau Sandstone outcrops.

The main results are as follows:

- 1) S_{grm} values are very scattered, from 5% to 85%, when porosity ranges from 6 to 24%.
- 2) S_{grm} versus porosity plots show three major trends:
 - Two very different but clear trends in the low to medium porosity range (below 14%). As porosity decreases, S_{grm} increases for Fontainebleau sandstone whereas it decreases for the other sandstones.
 - The third trend is in the high porosity region where the above two trends merge to an average of around 25-35%.
- 3) There is no clear relationship between S_{grm} and grain density, formation factor, cementation factor, or clay type.
- 4) The amount of clay is the controlling factor in the S_{grm} versus porosity relationship. In the low porosity region, the clay-free Fontainebleau sandstone traps much more gas than the shaly reservoir samples. For shaly sandstone, the greater the clay content, the lower the S_{grm} .

INTRODUCTION

During depletion of gas fields, the aquifer often encroaches into the reservoir, and residual gas saturation (S_{gr}) is used to estimate microscopic recovery. Published values of S_{gr} vary between 15 and 80%. The economic impact of S_{gr} on gas reservoirs can be extremely high. This is even more crucial for heterogeneous reservoirs where assessing S_{gr} for different rock types is the key issue.

Many studies have attempted to understand gas-trapping mechanisms. First, Geffen (1952) established that residual gas saturation measured in the laboratory on core plugs is the same as in a gas reservoir. Crowell (1966) illustrated the effect of initial gas saturation (S_{gi}) on trapped gas saturation (see also MacKay, 1974 and Jerauld, 1996). Land (1971) first proposed a characteristic shape for the relationship between S_{gi} and S_{gr} :

$$C = \frac{1}{S_{gr}^*} - \frac{1}{S_{gi}^*} = \frac{1}{S_{grm}} - 1.$$

Parameters are: S_{gi}^* that is effective initial gas saturation, expressed as fraction of the pore volume excluding the pore volume occupied by the irreducible wetting phase, S_{gr}^* that is effective residual gas saturation, expressed as fraction of the pore volume excluding the pore volume occupied by the irreducible wetting phase, and C that is Land coefficient.

The effect of water flooding rates on S_{gr} was found to be negligible (Geffen, 1952; Crowell, 1966; Delclaud, 1991). Katz (1966) showed that the residual gas left behind the moving water front remains constant and equal to that obtained during the measurement of capillary pressure. Several authors demonstrated that S_{gr} obtained by water flooding and spontaneous imbibition are very close (Geffen, 1952; Crowell, 1966; MacKay, 1974), provided the reduction in S_{gr} due to diffusion is disregarded (Delclaud; 1991). The type of displacing liquid was also found to be negligible in effect (Geffen, 1952; KYTE, 1956; Jerauld, 1996). The same S_{gr} values were obtained whatever the pressure and temperature prevailing during the core test (Geffen, 1952; Chierici, 1963; MacKay, 1974; Delclaud, 1991).

The results mentioned above prove that simple experimental conditions may be representative of gas trapping in reservoirs. As the objectives of this study are to gather a large number of experimental results over a large range of rock characteristics, simple experimental conditions are preferable. In this work, trapped gas saturations are obtained by spontaneous imbibition at ambient conditions on dry samples.

Many studies have tried to correlate trapped gas saturation to reservoir characteristics.

Chierici (1963) presented S_{gr} results obtained on 251 small samples of different lithological type: sand, sandstone, and bioclastic limestone plugs. S_{grm} values ranged from 10 to 31 percent. He failed to correlate S_{gr} values with porosity, permeability or irreducible water saturation. Attempts to correlate S_{gr} with distribution of pore entry radius and several combinations of porosity and permeability were also unsuccessful.

Katz (1966) presented a very general relationship between gas saturation and porosity on sand and sandstone cores. S_{gr} decreased from 50 to 10% when porosity increased from 10 to 40%. He did not find any trend against permeability.

MacKay (1974) reported S_{gr} values ranging from 24 to 44% on sandstone cores. He showed a very weak relationship between porosity and S_{gr} .

Keelan (1975) presented S_{gr} results for various carbonate types. Values range from 20 to 70%. Correlations between S_{gr} and porosity, permeability, combination of the two, initial gas saturation, pore entry distribution, images of thin section, and photomicrograph were sought. He concluded that S_{gr} increased as porosity decreased but no relationship with permeability was found. In a sandstone reservoir study, Keelan (1976) presented S_{gr} values from three reservoirs ranging from 32 to 45%, and concluded that S_{gr} increases slightly as permeability decreases.

Batycky (1981) presented a compilation of S_{gr} on carbonate rocks. The values vary from 40 to 70%.

Delclaud (1991) illustrated the wide variation of Sgr and its strong dependency on porosity for a North Sea gas field.

Jerauld (1996) studied Prudhoe Bay sandstone and conglomerate with porosity ranging from 13 to 25%. Maximum Sgr varies from 22 to 32%. He concluded that the maximum trapped gas saturation depends primarily on porosity, grain sorting, and microporosity. For sandstone, low porosity and poor sorting results in larger trapped gas levels. He also found a significant decrease in Sgrm with rising clay content. Conglomerates have, on average, a lower level of trapped gas at a given porosity level than sandstone. SEM photographs confirm the pore size to pore throat ratio as explanation of the gas trapping variation.

This short review shows that attempts to correlate Sgr with petrophysical characteristics have either failed or found a relationship against porosity. Figure 1 shows Sgrm versus porosity. It combines the results mentioned above and those of several other studies (Bousquié, 1979; Aissaoui, 1983; Fishlock, 1986). It illustrates a very general trend of increasing Sgr with decreasing porosity.

The present work studies relationships between maximum trapped gas saturation on the one hand and sandstone characteristics: porosity, permeability, grain density, formation factor, cementation factor, mineralogical data, clay contents and type on the other hand.

EXPERIMENTS

Core Samples

Samples were selected from three gas reservoirs, two from the Far East (M1 and M2) and one from West Africa (I3), and from Fontainebleau Sandstone outcrops (FTB). Their porosity and permeability range respectively from 6% to 25% and from 0.1 to 3 000 mD. Figure 2 illustrates porosity versus permeability. The samples' clay contents vary from 0 to 33%

Fontainebleau is 100% quartz, well-sorted sandstone, in which porosity is reduced due to quartz overgrowths around the grains as described by Bourbie (1985). The grain size is around 250 μm , with regular and plane surfaces and irregular geometric form. No noticeable variation in grain size is observed with porosity. The pores are of two main types: large, angular pores between quartz grains (radius of 10 to 30 μm), or very thin planar pores between two grains that represent an insignificant contribution to porosity. The SEM images show that decreasing porosity is directly related to decrease in relative volume of the large pores.

Reservoir sandstones contain primarily quartz grains, with variable amounts of cementation and other minerals (detrital clays, pyrites) along with bioclasts for some of the samples. Grain morphology varies from sub-angular to sub-rounded. Several types of grain surface are observed: planar and regular, altered, or irregular. The highest porosity values are those measured on samples composed of coarse-grained sand with little cementation. Porosity decreases as grain size decreases and cementation increases.

I3 sandstone contains clay laminations with bioturbation traces of varying intensity. Samples have a coarse pore structure, pores being located either between quartz grains, or as free space between cement and grains, or within interstratified minerals (illite,

illite/smectite, and smectite).

M1 and M2 sandstones have a grain size ranging from medium to very fine. Clays are scattered. Pore volume is either between quartz grains (radius of 5 μm), or as free space between cement and grains (radius about of 1 μm), as well as between cement minerals, or as space inside clays.

Cylindrical plugs of different lengths, and 23 mm or 40 mm in diameter were cut from whole core samples.

Maximum residual gas saturation (S_{grm}) measurement

The following sequence was performed. 1- Plugs were cleaned with chloroform by soxhlet extraction and dried at 80°C. 2- Matrix volume was measured either using helium pycnometry, or by hydrostatic weighing on chloroform-saturated samples 3- Bulk volume was measured by mercury hydrostatic weighing. 4- Gas permeability measurements. 5- Formation factor was measured on brine-saturated samples. 6- S_{grm} was measured as described in Figure 3.

Spontaneous imbibition of refined oil into a dry sample was used to obtain maximum trapped gas saturation. Isopar L was used as the invading wetting phase. Density, surface tension and viscosity at ambient laboratory conditions are 0.77 g/cm³, 1.38 cP and 24 .10⁻³ N/m respectively. Isopar L is used in order to carry out imbibition with strongly wetting liquid for both outcrop and reservoir samples. Oil spontaneous imbibition was performed by immersing the lowermost tip of the sample into oil and measuring the change of weight versus time. The sample was suspended from a hook underneath a balance as illustrated by figure 3. The major part of the sample remains immersed in air. Air remains saturated with liquid vapour as both the oil tank and the sample are in a closed system.

Change in oil saturation is calculated by mass balance, accounting for both the effect of buoyancy forces on the fraction of the sample immersed in oil and the effect of capillary forces along the perimeter of cylindrical sample. Trapped gas saturation is calculated from change in oil saturation as described below.

Change in gas saturation during imbibition is plotted against the square root of time. Figure 3 shows that two straight-line segments are usually observed: an early capillary-dominated period, followed by a late diffusion-dominated period. The intersection of these two lines was selected as the trapped gas saturation. Throughout the experiments, these two regimes were always clearly observed regardless of the sample permeability, except for the very low porosity Fontainebleau samples (porosity = 4%). Results for these very tight Fontainebleau samples were discarded.

Measurements and observations

The different types of measurements are listed in table 1.

- Porosity, permeability, grain density, formation factor and cementation factor were measured on the same plugs as for S_{grm} measurements.
- Mineral composition and clay type by XRD analysis were carried out on plug off-cuts for M1 and M2, and on part of the plugs for I3 and FTB sandstone. XRD analysis is

done on minerals and on the fines fraction.

Observations on thin sections and photomicrography supplemented the measurements.

Three mineralogical analyses were performed on Fontainebleau sandstone with various porosities. They confirm the sample composition as 100% of quartz.

RESULTS

Relationship between trapped gas saturation and porosity

There is a fair relationship between porosity and S_{grm} for each sandstone belonging to the lower- or the uppermost S_{grm}/porosity trend of this work, as illustrated by figure 4.

Figure 5 compares the S_{grm}/porosity trends obtained by Aissaoui (1983), by Jerauld (1996) and in this work on Fontainebleau samples. Our results superimpose onto Jerauld's data. There is a slight discrepancy between our results and Aissaoui's data. This is ascribed to the procedure used by Aissaoui to measure S_{grm}. S_{grm} was achieved when saturation did not change over a 24 hours period. Consequently, Aissaoui's estimate of S_{grm} partially includes the diffusion period and is consequently lower than our estimates. The overall agreement between our results and Jerauld's and Aissaoui's data is deemed to corroborate the reliability of our laboratory procedures.

Figure 6 shows the relationship between porosity and maximum trapped gas saturation on the Fontainebleau, I3, M1 and M2 sandstones. It illustrates that:

- 1) S_{grm} values are very scattered: from 5% to 85%.
- 2) S_{grm} versus porosity relationships present three major trends:
 - Two very different but clear trends in the low and medium porosity range, i.e. below 14%. As porosity decreases, S_{grm} increases for Fontainebleau sandstone whereas it decreases for other sandstone.
 - Concerning the highest porosity values, i.e. above 14%, the two trends above merge around an average S_{grm} of 25%.

Very similar behaviour was observed for S_{grm} versus permeability trends (Figure 7). Figure 8 shows the comparison between literature and our porosity/S_{grm} trends. This figure illustrates that our Fontainebleau results are in very good agreement with literature data. On the other hand, the lowermost S_{grm}/porosity trend has never been clearly evidenced before.

In the following, we try to correlate S_{grm} with a combination of porosity and mineralogical data.

Influence of clays

Macrolithological description shows that samples belonging to the lowermost S_{grm}/porosity trend are very often shaly. Moreover, microphotographs (Figure 9) and mineralogical analysis (Figure 10 a) confirm that the Fontainebleau sandstone is effectively clay-free. The hypothesis was advanced that clay content controls the S_{grm} versus porosity trends.

Figure 10 highlights the influence of clay presence and content on trapped gas saturation for low and medium porosity samples. It confirms that none of the samples belonging to the lowermost trend is clay-free. Figure 10 (b) shows a very clear relationship between the clay amounts and the trapped gas saturation for all the reservoir samples: the larger the clay fraction, the lower S_{grm} .

Table 2 presents the regression coefficients between maximum trapped gas saturation on one hand, porosity, clay contents, illite and kaolinite content and combination of some of these factors on the other hand. It confirms that S_{grm} is controlled by two keys: porosity and clay content.

Clay type influence

Presence, type, structure and location of clays within the porous network are known to influence petrophysical characteristics (Wilson, 1977), such as permeability and irreducible water saturation.

We observed different clay types: illite, smectite, illite/smectite, kaolinite and chlorite. Table 3 lists our main observations. No correlation was found between S_{grm} and location or structure of clays.

Attempts to correlate S_{grm} with any of the clay types were unsuccessful, as illustrated by regression coefficients in table 2 and figure 11 (a and b). A weak trend was obtained between S_{grm} and kaolinite or interstratified clay contents for I3 sandstone: S_{grm} values decrease if kaolinite contents decrease.

Relationship with other petrophysical parameters

We also tried to correlate S_{grm} with other petrophysical characteristics such as grain density, formation factor, and cementation factor. Figure 12 does not present evidence of any clear trend between S_{grm} and these parameters.

DISCUSSION

Our results on sandstone samples show that S_{grm} varies from 5 to 85%, when porosity ranges from 6 to 24%. The very large scatter in S_{grm} illustrated by our results explains why attempts to find a single relationship between porosity and S_{grm} often failed in the past (Chierici, 1963). Clearly, S_{grm} cannot be predicted *a priori* using porosity or permeability only, or any usual combination of the two.

Our uppermost S_{grm} /porosity trend obtained on Fontainebleau sandstone is consistent with data in other literature as shown in figure 1. The lowermost S_{grm} /porosity trend has never before been clearly reported for sandstone. However, it should be noted that such trends have occasionally been mentioned but often disregarded (Katz, 1966). Evidence of decreasing S_{gr} with decreasing porosity has also been published by Bousquié (1979) on outcrop carbonate samples.

Finally, porosity and clay content seem to control two-phase S_{grm} . Our results show a decrease in trapped gas saturation with increasing clay content. This is consistent with Jerauld's results (1996), except that he reported an overall increasing trend of S_{grm} when porosity decreases.

Our results suggest that the difference in S_{grm} /porosity behaviour can be ascribed to clay presence. In the low porosity region, the clay-free Fontainebleau sandstone traps much more gas than the shaly reservoir samples. In the medium to high porosity region, Fontainebleau and clean reservoir samples trap nearly the same amount of gas. These observations suggest that trapping mechanisms differ in the high and low porosity regions depending on the amount of clay and the pore network geometry.

It is agreed that the main factors affecting trapping of the strongly non-wetting phase are pore-to-throat ratio, throat-to-pore coordination number, type and degree of heterogeneity and surface roughness (Wardlaw, 1978). The latter two mechanisms are deemed negligible for Fontainebleau: thin sections show that this sandstone is effectively very homogeneous and SEM observations do not show any surface roughness.

In Fontainebleau sandstone, variations in pore network topology with porosity are deemed to control gas-trapping. Aissaoui (1983) distinguished two types of pores, depending on pore throat dimension. Our own observations confirm this pore typing. He noticed that the pore throat sizes diminish with porosity. This suggests that the variation with porosity of the ratio between pore body and pore throat is responsible for gas trapping. This explanation is consistent with the trapping behaviour in individual pores obtained by Wardlaw on glass micro-models (1982). Further work is required to support this hypothesis on Fontainebleau sandstone.

In our reservoir sandstone, the presence of clay results in low S_{grm} . This suggests that the microporosity within clay structures does not trap gas. The rationale behind this assumption is based on several mechanisms: low body-to-throat aspect ratio for most clay types, gas diffusion from microporosity to effective porosity due to the very high capillary pressure within the microporosity (Jerauld, 1996). Bousquié (1979) also concluded that microporosity does not trap gas on outcrop carbonate samples. He defined microporosity from mercury injection curves, as the fraction of the pore volume accessible by pore throats smaller than 1 μm .

However, it should be noted that this assumption has never before found clear corroboration. An extensive laboratory programme has recently been devoted to this issue and results are presented in a companion paper (Hamon, 2001).

CONCLUSION

- 1) S_{grm} values are very scattered, from 5% to 85%.
- 2) S_{grm} versus porosity plots show three major trends:
 - Two very different but clear trends in the low to medium porosity range, i.e. below 14%. As porosity increases, S_{grm} decreases for Fontainebleau sandstone whereas it increases for other sandstones.
 - Concerning the highest porosity values, i.e. above 14%, the two trends above merge around an average S_{grm} of 25%.
- 3) S_{grm} cannot be predicted a priori using porosity or permeability only, or any usual combination of the two.
- 4) There is no clear relationship between S_{grm} and grain density, or formation factor, or

cementation factor.

5) The amount of clay controls the S_{grM} versus porosity relationship. S_{grM} decreases as the clay content increases. No relationship was found between S_{grM} and the type of clay or location within the porous network.

NOMENCLATURE

C: Land coefficient	Phi: porosity (fraction of bulk volume)
clays: clay contents (weight fraction)	S_{gi}^* : effective initial gas saturation.
FTB: Fontainebleau sandstone	S_{gr}^* : effective residual gas saturation.
illite: illite fraction of clays (percent)	S_{gi} : initial gas saturation
kaolinite: kaolinite fraction of clays (percent)	S_{gr} : residual gas saturation
K_g : gas permeability (mD)	S_{grM} : maximum residual gas saturation

ACKNOWLEDGEMENTS

This paper is published with the permission of TotalFinaElf, Gaz De France and the Ecole des Mines de Paris. We thank S. Bouzida, J.B. Vignal and L. Menard for their contribution.

REFERENCES

- Aissaoui A., *Etude théorique et expérimentale de l'hystérésis des pressions capillaires et des perméabilités relatives en vue du stockage souterrain de gaz*, Thesis Ecole des Mines de Paris (1983), 223 p
- Batycky, J., Irwin, D., Fish, R., "Trapped gas saturation in Leducage reservoirs", *Journal of Canadian Petroleum Technology*, (Feb 1998), v 37, n 2, pp 32-39
- Bourbie T., Zinszner B., "Hydraulic and acoustic properties as a function of porosity in Fontainebleau sandstone", *Journal of Geophysical Research*, (1985), v 90, b13, pp 11.524 -11.532,
- Bousquié P., *Texture et porosité de roches calcaires*, Thesis Ecole des Mines de Paris (1979), 191 p
- Chierici G.L., Ciucci G.M., Long G., "Experimental research on gas saturation behind the water front in gas reservoirs subjected to water drive", *Proc. of the World Petroleum Congress, Frankfurt am Main*, (June 1963) sec II, paper 17, PD6, pp 483-498
- Crowell D.C., Dean G.W. Loomis, "Efficiency of gas displacement from a water-drive reservoir", *Report of investigations 6735 USBM*, (1966), pp 1- 29
- Delclaud J., "Laboratory measurements of the residual gas saturation", *Second European Core Analysis Symposium* (20-22 May 1991) London, pp 431-451
- Fishlock T.P., Smith R.A., Soper B.M. Wood R.W., "Experimental studies on the waterflood residual gas saturation and its production by blowdown", *SPE 15455 presented at 61st annual technical conference and exhibition of SPE, New Orleans*,(1988), v 3, n 2, pp 387-394 .
- Geffen T.M., Parish D.R., Haynes G.W., and Morse R.A., "Efficiency of gas displacement from porous media by liquid flooding", *trans. AIME presented at the fall meeting of the petroleum branch in Oklahoma City Okla.*, (1952), v 195, pp 29-38
- Hamon G., Suzanne K., Billiotte J., Trocme V., "Field-wide variations of trapped gas saturation in heterogeneous sandstone reservoirs", *SPE 71524*, (2001), 30 Sept. to 3 Oct. 2001 in New Orleans, USA.
- Jerauld G.R., "Gas-oil relative permeability of Prudhoe bay", *SPE 35718 presented at the western regional meeting held in Anchorage, Alaska*, (1996), pp 653-670.
- Katz D.L., Legatski M.W., Tek M.W., Gorring M.R., Neilsen R.L., "How water displaces gas from

porous media”, *Oil and Gas Journal* (Jan., 1966), pp 55-60

- Keelan D.K., “A practical approach to determination of imbibition gas-water relative permeability”, *SPE 4988 presented at the SPE-AIME 49th annual fall meeting held in Houston*, (Feb. 1976), pp 199-204
- Keelan D.K., Dugh V.J., “Trapped-gas saturation in carbonate formations”, *SPE 4535 presented at the SPE-AIME 48th annual fall meeting held in Las Vegas*, (April 1975), pp 149-160
- Kyte J.R., Stanclift R.J., Stephan S.C., Rapoport L.A., “Mechanism of water flooding in the presence of free gas”, *J. Pet. Tech. Trans AIME*, (sept1956), v **195**, pp 322-323
- Land C.S., “Comparison of calculated with experimental imbibition relative permeability”, *SPE 3360 presented at the Rocky Mountain regional meeting, Billings, MT*, (Dec. 1971), pp 419-425
- Mc Kay B.A., “Laboratory studies of gas displacement from sandstone reservoirs having strong water drive”, *APEA Journal*, (1974), pp 189-194
- Wardlaw N.C. , “The effects of geometry, wettability, viscosity and interfacial tension on trapping in single pore-throat pairs”, *Journal of Canadian Petroleum Technology, Reservoir Engineering*, (May-June 1982), pp 21-27
- Wardlaw N.C., Cassan J.P., “Estimation of recovery efficiency by visual observation of pore systems in reservoir rocks”, *Bull Can Petrol Geology*, (1978), v **26**, n **4**, pp 572-585
- Wilson M.D., Pittman E.D., “Authigenic clays in sandstones: recognition and influence on reservoir properties and paleoenvironmental analysis”, *Journal of Sedimentary Petrology*, (1977), v **47**, n **1**, pp 3-31

TABLES

Sandstone	Petrophysical and Sgrm measurement	XRD analysis	Thin sections	Photo micrography
FTB	63	3	10	4
I3	54	31		2
M1	145	51	38	6
M2	100	47		3
total	362	129	48	15

Table 1: Number of measurements

R^2	Phi		Clays	Illite	Kaolinite	Formula	R^2
	parabolic	linear					
<i>I3</i>	0.49	0.32	0.68	0	0.3	1.18 Phi – 0.86 Clays + 0.22	0.74
<i>M1</i>	0.76	0.56	0.68	0.1	0	0.97 Phi – 1.39 Clays + 0.27	0.74
<i>M2</i>	0.69	0.68	0.37	0.1	0.1	1.83 Phi – 0.12 Clays – 0.03	0.70
<i>I3 + M1 + M2</i>	0.52	0.40	0.61	0.25	0.21	1.02 Phi – 1.04 Clays + 0.24	0.70

Table 2: Correlation between Sgrm and petrophysical and mineralogical parameters on plug with XRD analysis

clays – type	Structure // Microporosity	Location within pore network		
		I3	M1	M2
Illite, illite-smectite, smectite	Sheet of elongate spines (+++)	Pore filling	Pore lining and filling	Pore lining and filling
Kaolinite	Stacked plates (+)	Pore filling	Pore filling	Pore filling
Chlorite	Honeycomb (+++)	None	-	Pore lining

Table 3: Structure and location of clays

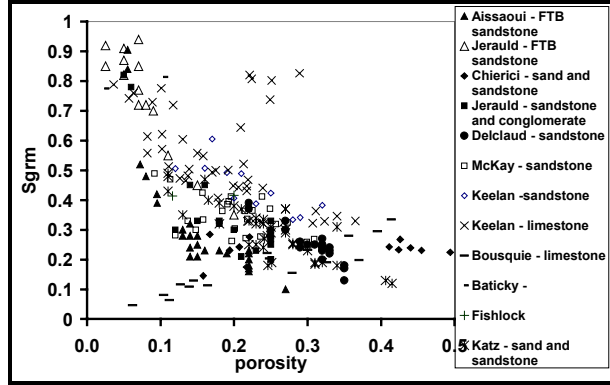


Figure 1: Literature data on maximum trapped gas saturation versus porosity

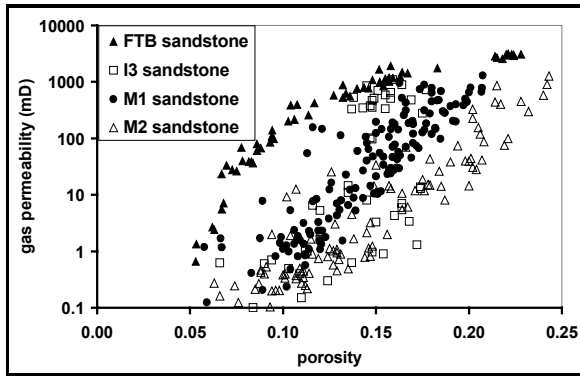


Figure 2: Porosity against permeability

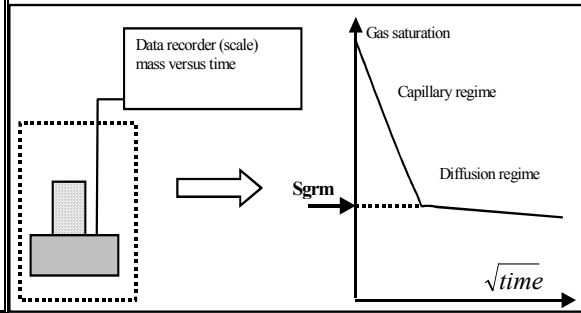


Figure 3: Principle of measurement of Sgr

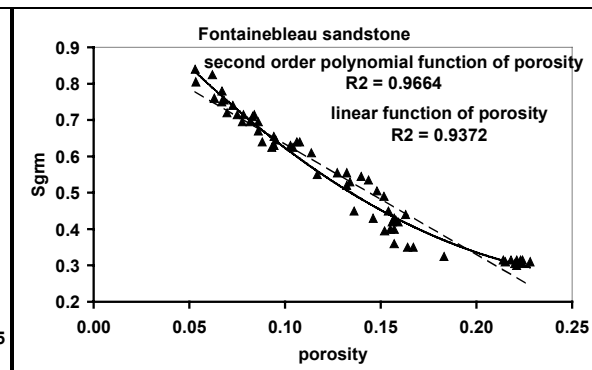
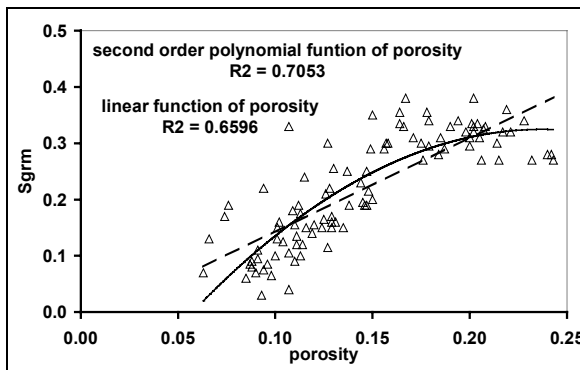


Figure 4: Sgrm versus porosity for M2 (4a) and Fontainebleau sandstone (4b)

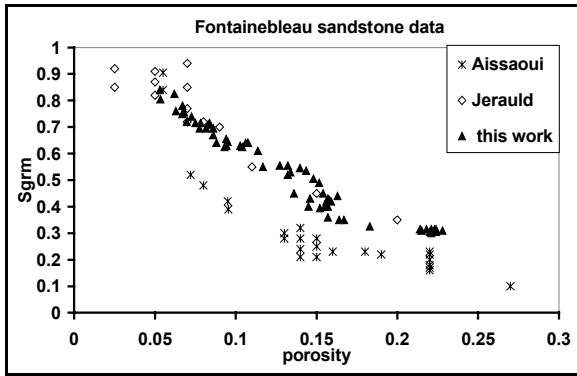


Figure 5: Sgrm versus porosity for Fontainebleau sandstone, literature and our data

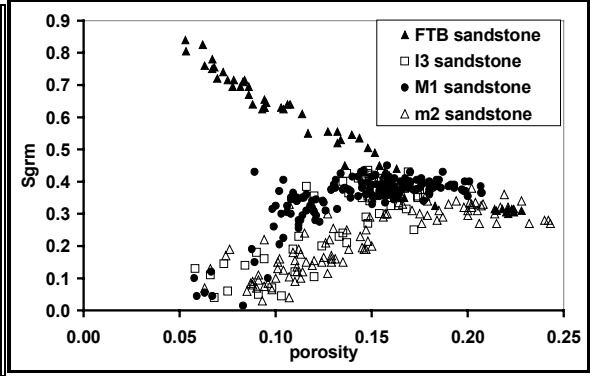


Figure 6: Sgrm versus porosity for Fontainebleau sandstone and all samples.

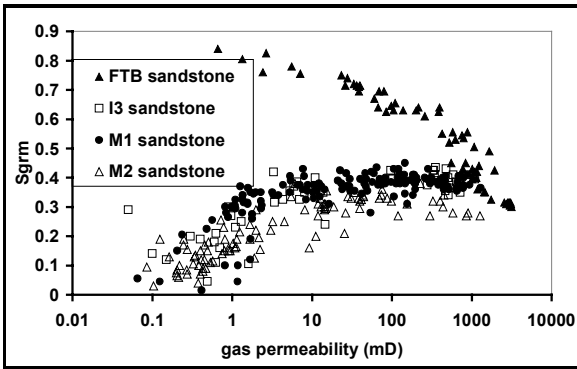


Figure 7: Gas permeability versus Sgrm

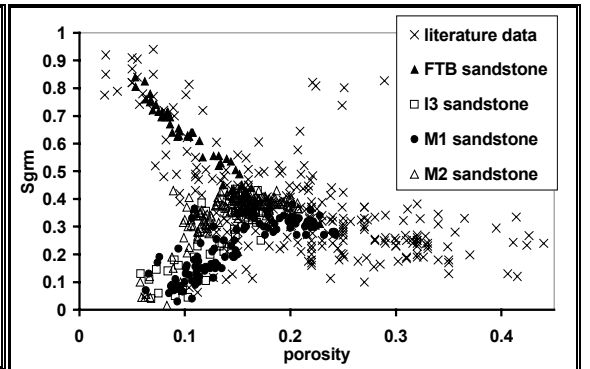


Figure 8: Porosity versus Sgrm, literature and our data

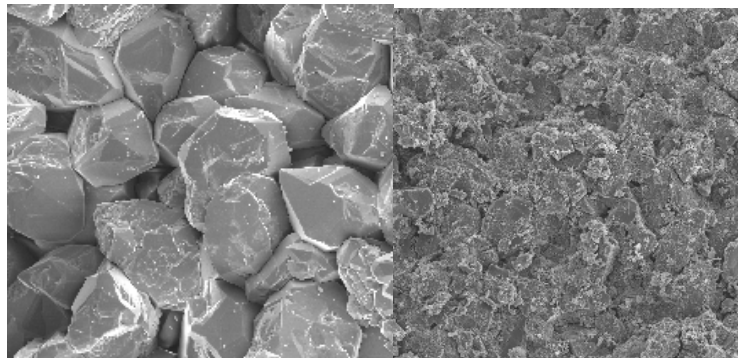


Figure 9: SEM images of Fontainebleau sandstone and reservoir sandstone (Phi = 9% - *100)

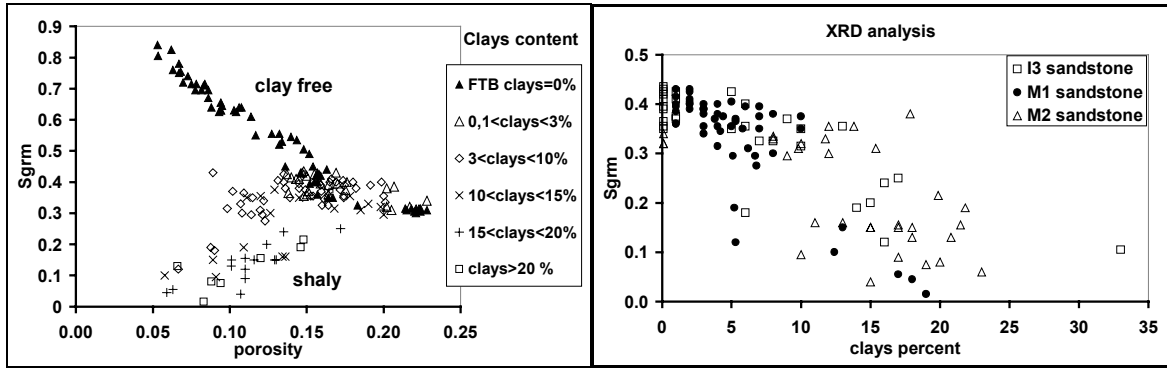


Figure 10: Influence of clay presence (10a) and Sgrm versus clay content (10b)

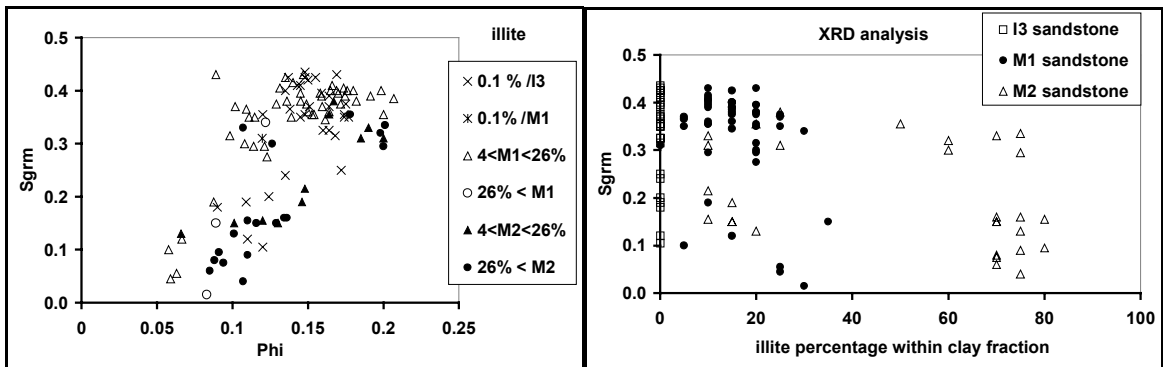


Figure 11: Influence of illite percentage (within clay fraction) on trapped gas (11a) and Sgrm versus illite contents (11b)

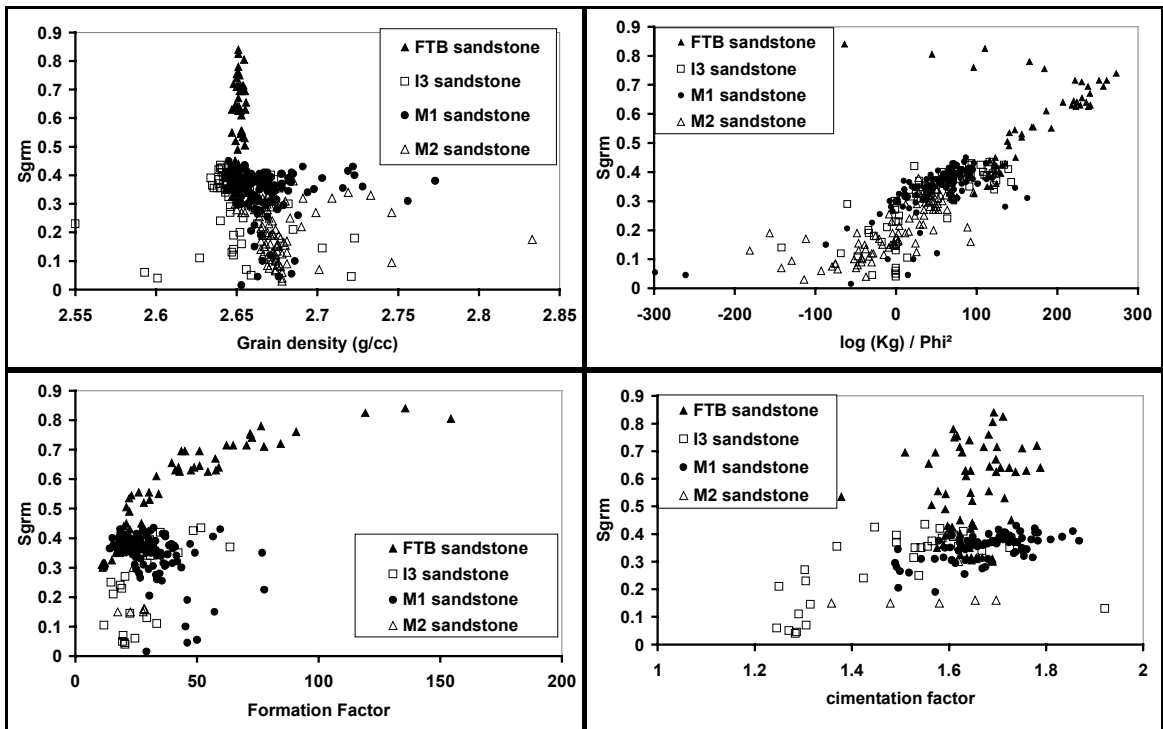


Figure 12: Trapped gas as a function of petrophysical parameters.